

MS BOLA YOON (Orcid ID : 0000-0002-6087-5373)

PROFESSOR PANKAJ SARIN (Orcid ID : 0000-0001-9110-7660)

DR RISHI RAJ (Orcid ID : 0000-0001-8556-9797)

Article type : Rapid Communication

Corresponding author mail id :-

rishi.raj@colorado.edu

## On the Synchronicity of Flash Sintering and Phase Transformation

Bola Yoon<sup>1</sup>, Devinder Yadav<sup>1,2</sup>, Sanjit Ghose<sup>3</sup>, Pankaj Sarin<sup>4</sup> and Rishi Raj<sup>1</sup>

<sup>1</sup>Materials Science and Engineering Program, Department of Mechanical Engineering, University of Colorado Boulder, Colorado

This is the author manuscript accepted for publication and has undergone full peer review but has not been through the copyediting, typesetting, pagination and proofreading process, which may lead to differences between this version and the [Version of Record](#). Please cite this article as [doi: 10.1111/JACE.16335](https://doi.org/10.1111/JACE.16335)

This article is protected by copyright. All rights reserved

<sup>2</sup>Department of Metallurgical and Materials Engineering, Indian Institute of Technology Patna, Bihar, India

<sup>3</sup>National Synchrotron Light Source II, Brookhaven National Laboratory, Upton, New York

<sup>4</sup>School of Materials Science and Engineering, Oklahoma State University, Tulsa, Oklahoma

Submitted as a Rapid Communication to the Journal of the American Ceramic Society (Second Revision)

## Abstract

There is growing evidence that oxides of complex chemistries can be formed in one step by reactive flash sintering of their elemental constituents. Here we explore the temporal relationship between phase transformation and sintering by combining measurements of sintering with *in-situ* measurements of phase transformation. The experiments are carried out under current-rate, where flash is induced by injecting current and increasing it at a constant rate. We show that phase transformation of powders of magnesia and  $\alpha$ -alumina into single-phase magnesium aluminate spinel was completed in 45 s, whereas sintering to full density required 60 s.

## 1. Introduction

The discovery of flash sintering<sup>1</sup> is evolving into a process for the synthesis of multi-constituent ceramics that are difficult to make by conventional methods. Powders of elemental components can be mixed and flashed in mere seconds to produce single-phase oxides of complex

compositions.<sup>2-5</sup> The phase transformation and sintering occur concomitantly. We call this process reactive flash sintering.

The question arises if the two processes, phase transformation and sintering, occur together or whether one precedes the other. In this article we seek to measure the relative rates of phase transformation and sintering for the following reaction<sup>4, 5</sup>



Our approach is to synchronize the rate of sintering with the rate of phase transformation in live experiments at the NSLS-II Synchrotron. These experiments are made possible by a new method called current-rate flash, where the process is carried out entirely under current control.<sup>6</sup> The time-span of the reaction can now be stretched by changing the rate of current increase since the extent of the reaction depends not on the current-rate but rather on the instantaneous value of the current density.<sup>6</sup> For example, it was shown that the duration of flash sintering could be stretched from 7 s to 700 s by changing the current rate<sup>6</sup> (in the traditional voltage to current flash experiments the process is completed in < 5 s<sup>1</sup>) The longer duration is needed for time dependent measurements of the phase transformation at the XPD synchrotron beamline of NSLS-II, due to limited large 2D detector speed and efficiency, which limits the scan rate to about 0.5 - 1.0 Hz.

## 2. Experimental: Materials and Methods

### 2.1 Materials

Stoichiometric mixture of Al<sub>2</sub>O<sub>3</sub> (AKP-50, 0.2 µm, Sumitomo Chemical, Japan) and MgO (99.9%, 1 µm, Inframet Advanced Materials, CT) were mixed with 50 vol% of yttria (8 mol%) stabilized zirconia (8YSZ, TZ-8Y, 25 nm, Tosoh USA, OH).

8YSZ serves as a catalyst for inducing the flash in materials which otherwise could not be flashed within the limits of the power supply currently available to us.

The sintering experiments were carried out on dog-bone shaped specimens using a conventional furnace fitted with an optical system for measurement of shrinkage of the gage section from photographs taken at regular intervals. The long gage length (15 mm) of these specimens was needed to obtain good measurements of the shrinkage.

The Synchrotron experiments for measurement of phase transformation were carried out with rectangular bars that were thin enough (0.8 mm) for the X-ray beam to travel through the thickness of the specimens in order to obtain measurements of phase changes within the bulk of the specimen. These specimens and the special furnace have been designed for the X-ray stage at NSLS-II. The gage length of these specimens (<4 mm) was not enough to obtain good measurements of shrinkage by the optical method described above.

## 2.2 Sintering Experiments

The powder mixture was pressed in a dog-bone shaped die, which has a gage-section of 15 mm × 3.5 mm × ~1.3 mm (the thickness varied slightly since it depended on the amount of powder placed in the die and the pressure used to press it). A 3 kW DC power supply (Glassman High Voltage Inc., NJ) and a Keithley multimeter were used. The linear shrinkage of the sample was monitored through a CCD camera with optical filters, using equation  $\varepsilon = \ln(l/l_0)$ , where  $l_0$  is initial gage length and  $l$  is the time dependent gage length. Final density was determined using the equation:  $\rho = \rho_g e^{-3\varepsilon}$ , where  $\rho_g$  is the green density.<sup>7</sup> The green density was measured from the weight and the volume of the die-pressed sample. Theoretical density of the composite is 5.09 g cm<sup>-3</sup>. The green density of dog-bone shape sample was measured from the weight and the volume of the sample, which were 0.1731 g and 0.06786

cm<sup>3</sup>, respectively, which yields a relative green density of  $\rho_g = 0.50$ , as calculated from the equation just above.

The flash sintered specimen was polished and thermally etched at 1100°C for 1 h. The microstructures were characterized by a scanning electron microscope (SEM, SU-3500, Hitachi, Japan). The average grain size was measured by the linear intercept method.

### 2.3 In-situ X-ray Diffraction Experiments

The powder mixture was pressed into rectangular bars, ~4 mm long with a cross section of 1.6 mm × 0.8 mm. The specimens were subjected to binder burn-out at 600°C for 1 h with a heating rate of 2 °C min<sup>-1</sup>. They were pre-sintered by heating up to 900°C at 10 °C min<sup>-1</sup> and holding for 1 h. Platinum wires, 0.25 mm in diameter, were wrapped to the ends of the bar; they served as the electrodes.

Synchrotron X-ray diffraction experiments were performed at the beamline XPD 28ID-2 of the National Synchrotron Light Source II (NSLS II) at Brookhaven National Laboratory.<sup>8</sup> The monochromatic X-ray energy used for this measurement was 66.408 keV ( $\lambda=0.1867$  Å). Raw two-dimensional patterns were integrated to one-dimensional powder diffraction patterns using Fit2D software.<sup>9</sup> The area under the diffraction peaks was measured using a *Pseudo-Voigt* equation. PDF files for ZrO<sub>2</sub> (JCPDS 81-1551), Al<sub>2</sub>O<sub>3</sub> (JCPDS 85-1337), MgO (JCPDS 78-0430) and MgAl<sub>2</sub>O<sub>4</sub> (JCPDS 86-0096) were used for peak indexing.

The details of the setup for *in-situ* experiments at NSLS II are described in<sup>10, 11</sup>. The electric field was applied from a DC power source (Sorenson 300-2, Sorenson, CA) and the current was measured with a digital multimeter (Keithley 2000, Keithley Instruments, OH).

### 2.4 Synchronization of Current-Rate Experiments

Both the sintering and the synchrotron experiments were carried out at the same current rate. The target current rate was set at 100 mA mm<sup>-2</sup>

$\text{min}^{-1}$  using the initial value of the cross section for describing the current density. The current limit was set at  $100 \text{ mA mm}^{-2}$ , so that the total duration of the experiment was 60 s.

A plot of the increase in current density with time is shown in Fig. 1. The slight step, early on, is from the incubation time for the onset of the flash, which led to a mild discrepancy between the target and the actual current rate. Thus, in this instance, while the target current rate was  $100 \text{ mA mm}^{-2} \text{ min}^{-1}$ , the actual value averaged over the span of the experiment was  $128 \text{ mA mm}^{-2} \text{ min}^{-1}$ . The incubation time varies from one experiment to another which causes slight differences in the current rates. In all instances the current rate was adjusted so that the current limit of  $100 \text{ mA mm}^{-2}$  was reached in 60 s. In any event, the results in the current rate experiments depend on the instantaneous value of the current density, not its rate<sup>6</sup>; therefore, the variability in the current rate can be discounted by plotting the results in terms of the current density, rather than time.

## 2.5 Measurement of Temperature

The temperature was measured with the platinum standard during the live synchrotron experiments.<sup>11</sup> A thin line of platinum-paste, less than 1 mm wide was applied with a fine brush on the surface of the specimen was applied to the surface of the sample. The platinum line was aligned normal to the current flow through the gage section, and placed such that the X-ray beam would pass through it. The calibration was done by heating the specimen up to  $1500^\circ\text{C}$  without applying electric field, and measuring the shifts in the (111) and (200) peaks of platinum which were related to temperature via the handbook data for thermal expansion of Pt.<sup>12</sup> A complete description is included in Supplementary Materials.

The temperature was also estimated from the black body radiation (BBR) model where the electrical power density is equated to the radiation loss to obtain the specimen temperature.<sup>13</sup> The radiation loss depends on the emissivity. The emissivity of alumina and spinel are

quite different, therefore the emissivity in the BBR model was adjusted as spinel grew at the expense of alumina. The equations and the procedure for applying the BBR model are described in<sup>4, 13</sup>. A full discussion is included in Supplementary Materials.

The experiments were carried out with the furnace thermocouple set at 900°C. However, the specimen temperature was measured to be 960°C with the platinum standard. We use this latter temperature for the BBR model. This difference is due to the position of the thermocouple, because if placed in the center of the hot zone it would have interrupted the X-ray path.

### 3. Results

#### 3.1 Synchronicity

The main objective of this study was to determine the temporal relationship between phase transformation and sintering during reactive flash sintering of Al<sub>2</sub>O<sub>3</sub> and MgO to form single-phase MgAl<sub>2</sub>O<sub>4</sub> spinel.

The time dependent emergence of spinel and dissolution of alumina are shown in Fig. 2. For example, the (111) peak for alumina weakens while the (111) peak for spinel strengthens. Same behavior is seen in the decline of the (-210) peak of alumina, as well as the decline in the (200) peak for MgO, along with the rise in the (311) spinel peak. The phase transformation is complete within 45 s. Quantitative measurements of the phase transformation were obtained from the reduction in the area under the (111) alumina-peak. The progression of the phase transformation can be seen in the video, attached as Supplementary Material (S1\_Spinel.mp4).

In Fig. 3 the results for sintering and phase transformation are plotted both as a function of time and the current density. We note that whereas the phase transformation is essentially complete in 40 – 45 s, ~60 s are required to complete sintering, that is, sintering

lags phase transformation by 10 - 15 s. An equivalent lag is seen when the data are plotted against the current density, affirming that phase transformation precedes sintering.

### 3.2 Microstructure

The microstructure across the entire width of the specimen is given in Fig. 4. The dark phase corresponds to spinel and the bright phase to zirconia. The final density of the specimen is 97%, with no obvious residual alumina and magnesia phases. The grain size is remarkably uniform across the entire gage section of the specimen, even close to the electrodes. A similar finding was reported in current rate experiments with 3YSZ.<sup>6</sup>

Usually, the grain size becomes non-uniform, with evidence of redox reactions near the electrodes.<sup>14-16</sup> The voltage expressed at the electrode is equal to the product of the current density and the interfacial resistance. There is growing evidence that the metal-ceramic interfaces become non-blocking for electron transfer under flash conditions.<sup>17, 18</sup> The highest voltage across the interface is equal to the product of the current density and the interfacial resistance. In the voltage-to-current experiments the surge in current<sup>19</sup> at the onset of flash can cause the voltage to rise above electrolytic decomposition values. We explain the uniform grain size in current rate experiments by the initiation of flash at very low current densities<sup>6</sup>, which are insufficient to induce electrolytic decomposition at the electrodes.

### 3.3 Temperature

The temperature of the specimen was measured with the platinum standard at NSLS-II, and estimated by the BBR model. The procedures are fully described in earlier publications,<sup>4, 11</sup> and in Supplementary Materials, as well.

The shifts in the Pt peaks during live flash experiments were measured to determine the thermal expansion, which could then be related to the specimen temperature as described earlier in this article.

The BBR estimate relies on the value of emissivity which on average decreases with the growth of spinel, which has a lower emissivity (0.2) than alumina (~0.47). We use the rule of mixtures to estimate the emissivity of the composite when alumina transforms into spinel. The BBR model also requires knowledge of the surface to volume ratio of the sample, which changes as the sample shrinks; this ratio was calculated from shrinkage measurements. The other parameters in the model are the electrical power dissipation and the furnace temperature. With the values of all these parameters in hand the BBR model<sup>13</sup> can be used to estimate the specimen temperature.

The caveat in the above approach is that the BBR model assumes a steady state specimen temperature such that black body radiation is equal to the electrical power dissipation. If the specimen temperature changes then some of the energy input is absorbed in specific heat. This issue has been fully addressed in Ref.<sup>6</sup>. If the current rates are slow, as the one used in the present experiments, the correction has been shown to be minor.<sup>6</sup>

The BBR model prediction is compared to the measurement with the platinum standard in Fig. 5. The experimental measurement of temperature is definitely lower than the BBR estimate. We hypothesize that this extra energy is expended in a process other than black body radiation. Recent results from a molecular dynamics model by Jongmanns et al.<sup>20</sup> show that significant input energy may be consumed in the formation of Frenkel defects.

#### 4. Discussion

The principal objective of the present experiments was to determine the temporal relationship between sintering and phase transformation during reactive flash sintering. This study was made possible by

current-rate experiments where the span of the sintering experiment can be stretched in time simply by using a slower current-rate. The slower rate allowed us to obtain X-ray scans for the development of the spinel phase from magnesia and alumina at NSLS-II. The current rate was designed for the experiment to be completed in 60 s upon reaching a current density of  $100 \text{ mA mm}^{-2}$ .

The synchronicity of phase transformation and sintering was measured by combining sintering experiments with X-ray scans at NSLS-II. The data in Fig. 3 show that phase transformation was completed in  $\sim 45$  s, and sintering in 60 s.

The above finding is not unreasonable, since sintering requires chemical diffusion which is controlled by the slowest moving species. On the other hand, phase transformation would depend on the diffusion of the species that can produce the change in phase. Therefore, it is conceivable that the rate of phase transformation is less restrictive than sintering.

The present experiments with spinel, like the first experiments with current-rate with 3YSZ, show a highly uniform microstructure across the full gage section. This is an important finding since often in the voltage-to-current experiments the grain size near the electrodes is different than in the middle of the gage section.<sup>21</sup>

Finally, the results suggest an energy loss process other than black body radiation in current rate experiments. In this context, recent molecular dynamics results by Jongmanns et al.<sup>20</sup>, who have shown that significant energy can be absorbed in the creation of Frenkel defects, are significant.

## 5. Conclusions

Recent experiments, with bismuth oxide and ferric oxide to form bismuth ferrite<sup>2</sup>, and with reactions between alumina and magnesia to form spinel,<sup>4, 5</sup> have shown that phase transformations and sintering can

occur together during a flash experiment. Conventional sintering usually requires stoichiometric powders, adding significant cost to manufacturing. In reactive flash sintering elemental oxides can be used as the starting materials for the synthesis of single-phases of complex oxides.

The present experiments have been made possible by a recent discovery of current-rate controlled flash. Since the sintering behavior depends on the instantaneous value of the current density<sup>6</sup>, the span of the flash sintering can be stretched out to several seconds by using a slower current-rate. This longer span enabled the measurement of time dependent phase transformation during *in-situ* X-ray diffraction experiments. We show that phase transformation precedes sintering. This difference reflects on a different species controlling the overall kinetics of sintering and phase transformation.

The BBR model depends on the emissivity of the ceramic. The spinel case is particularly interesting since spinel has an emissivity that is significantly lower than alumina. As alumina transforms into spinel the average emissivity of the sample decreases producing a significant change in the BBR prediction.

Finally this is a second time where we show that the microstructure from current-rate flash sintering is more uniform across the gage section than is usually obtained in voltage-to-current experiments.<sup>6</sup> This difference is ascribed to the initiation of flash at much lower current densities in the current-rate experiments.

## Acknowledgements

This research was supported by a grant, W911NF-16-1-0200, from the Army Research Office, under the direction of Dr. Michael Bakas, and by Office of Science of the Department of Energy, Grant/Award Number: DE-AC02-98CH10886. This research used 28ID-2 (XPD) beamline of

the National Synchrotron Light Source II, a U.S. Department of Energy (DOE) Office of Science User Facility operated for the DOE Office of Science by Brookhaven National Laboratory under Contract No. DE-SC0012704. We gratefully acknowledge inputs from Dr. Jean-Marie Lebrun during the course of this investigation.

## References

1. Cologna M, Rashkova B, Raj R. Flash sintering of nanograin zirconia in <5 s at 850°C. *J Am Ceram Soc.* 2010;93:3556–3559.
2. Gil-González E, Perejón A, Sánchez-Jiménez PE, Sayagués MJ, Raj R, Pérez-Maqueda LA. Phase-pure BiFeO<sub>3</sub> produced by reaction flash-sintering of Bi<sub>2</sub>O<sub>3</sub> and Fe<sub>2</sub>O<sub>3</sub>. *J Mater Chem A.* 2018;6:5356–5366.
3. Avila V, Raj R. Reactive flash sintering: synthesis of dense single phase cubic alumino-lithium lanthanum zirconate from powders of Al<sub>2</sub>O<sub>3</sub>, Li<sub>2</sub>O, La<sub>2</sub>O<sub>3</sub>, and ZrO<sub>2</sub> at 650°C. Under Review. 2019.
4. Kok D, Yadav D, Sortino E, et al. α-Alumina and spinel react into single phase high-alumina spinel in < 3 seconds during flash sintering. *J Am Ceram Soc.* 2019;102:644–653.
5. Yoon B, Yadav D, Ghose S, Raj R. Reactive flash sintering: MgO and α-Al<sub>2</sub>O<sub>3</sub> transform and sinter into single-phase polycrystals of MgAl<sub>2</sub>O<sub>4</sub>. *J Am Ceram Soc.* In press 2018.
6. Kumar M, Yadav D, Lebrun J-M, Raj R. Flash sintering with current-rate: A different approach. *J Am Ceram Soc.* 2019;102:823–835.
7. Raj R. Separation of Cavitation-Strain and Creep-Strain During Deformation. *J Am Ceram Soc.* 1982;65(3):C-46.
8. Shi X, Ghose S, Dooryhee E. Performance calculations of the X-ray powder diffraction beamline at NSLS-II. *J Synchrotron Radiat.* 2013;20:234–242.
9. Hammersley AP, Svensson SO, Thompson A, Graafsma H, Kvick Å, Moy JP. Calibration and correction of distortions in two-dimensional detector systems. *Rev Sci Instrum.* 1995;66:2729–2733.

10. Yoon B, Yadav D, Raj R, et al. Measurement of O and Ti atom displacements in  $\text{TiO}_2$  during flash sintering experiments. *J Am Ceram Soc.* 2018;101:1811-1817.
11. Lebrun JM, Morrissey TG, Francis JSC, Seymour KC, Kriven WM, Raj R. Emergence and extinction of a new phase during on-off experiments related to flash sintering of 3YSZ. *J Am Ceram Soc.* 2015;98:1493-1497.
12. Hahn TA, Kirby RK. Thermal expansion of platinum from 293 to 1900 K. *AIP Conf Proc.* 1972;3:87-95.
13. Raj R. Joule heating during flash-sintering. *J Eur Ceram Soc.* 2012;32:2293-2301.
14. Biesuz M, Sglavo VM. Current-induced abnormal and oriented grain growth in corundum upon flash sintering. *Scripta Mater.* 2018;150:82-86.
15. Charalambous H, Jha SK, Wang H, Phuah XL, Wang H, Tsakalakos T. Inhomogeneous reduction and its relation to grain growth of titania during flash sintering. *Scripta Mater.* 2018;155:37-40.
16. Jha SK, Charalambous H, Wang H, et al. In-situ observation of oxygen mobility and abnormal lattice expansion in ceria during flash sintering. *Ceram Int.* 2018;44:15362-15369.
17. Wagner T, Kirchheim R, Ru"hle M. Electrochemically-induced reactions at Ni/ $\text{ZrO}_2$  interfaces. *Acta Metall Mater.* 1992;40:S85-S93.
18. Masó N, West AR. Electronic conductivity in yttria-stabilized zirconia under a small dc bias. *Chem Mater.* 2015;27:1552-1558.
19. Francis JSC, Raj R. Influence of the field and the current limit on flash sintering at isothermal furnace temperatures. *J Am Ceram Soc.* 2013;96:2754-2758.
20. Jongmanns M, Raj R, Wolf DE. Generation of Frenkel defects above the Debye temperature by proliferation of phonons near the Brillouin zone edge. *New J Phys.* 2018;20:093013.
21. Yoshida H, Biswas P, Johnson R, Mohan MK. Flash-sintering of magnesium aluminate spinel ( $\text{MgAl}_2\text{O}_4$ ) ceramics. *J Am Ceram Soc.* 2017;100:554-562.

## Figure Captions

Figure 1. The current density vs time in the current-rate controlled experiments at the Synchrotron - for phase transformation measurements - with rectangular bar shaped specimens, and sintering with dog-bone specimens.

Figure 2. (a) Electric field, current density and power density curves of the current-rate flash experiment. Onset of the flash is signaled by a peak of voltage, around 10 seconds. (b) In-situ X-ray diffraction data of the composite with corresponding points from 1 to 7 in (a).

Figure 3. Temporal relationship between sintering and phase transformation shown in terms of real time, and in terms of the increase in the current density with time.

Figure 4. (a) A schematic of dog-bone shape specimen and (b) the SEM images of corresponding points from #1 to #5; the grain size is given for each micrograph.

Figure 5. Power dissipation and specimen temperature estimated from the black body radiation model and in-situ measurements from platinum standard.

jace\_16335\_f1.eps

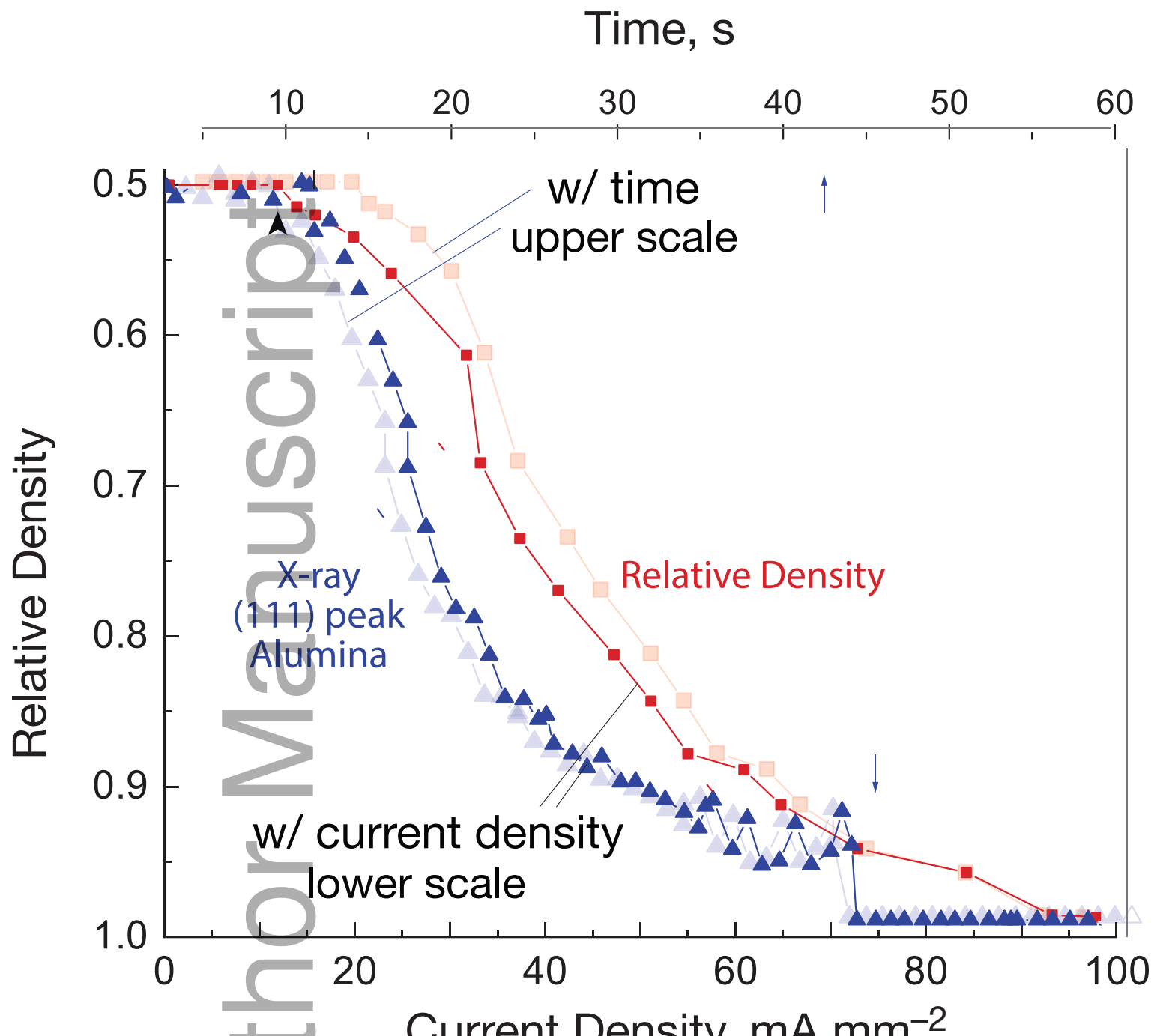
# Author Manuscript

This article is protected by copyright. All rights reserved

jace\_16335\_f2.eps

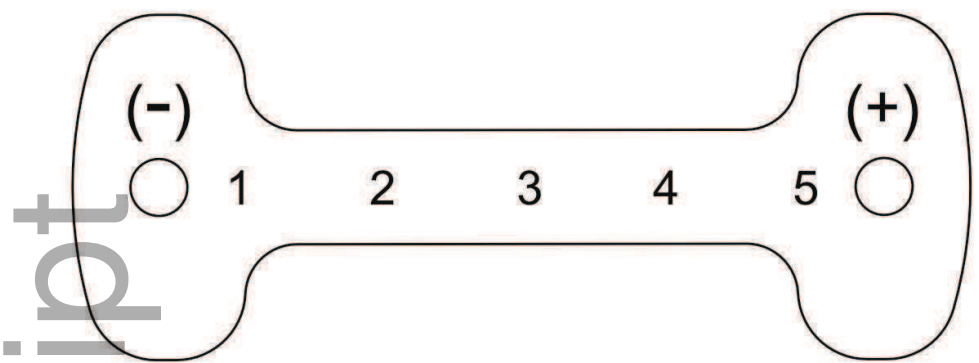
# Author Manuscript

This article is protected by copyright. All rights reserved



jace\_16335\_f3.eps

(A)



(B)

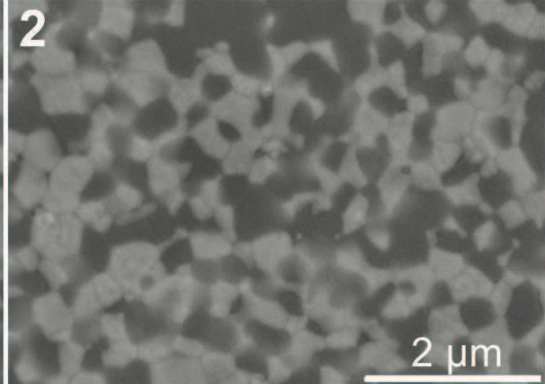
$341 \pm 11 \text{ nm}$

1



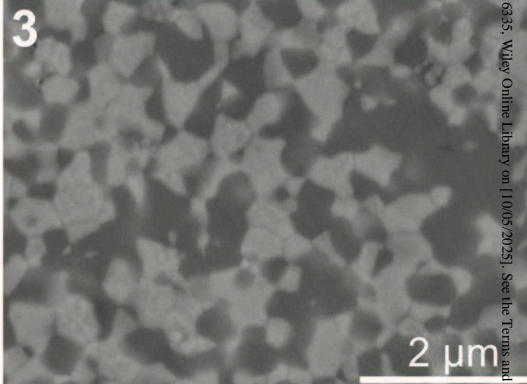
$339 \pm 7 \text{ nm}$

2

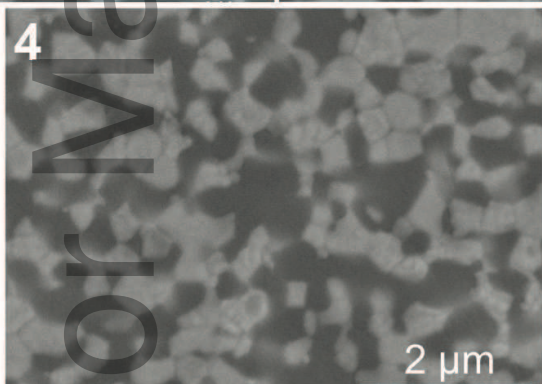


$335 \pm 8 \text{ nm}$

3

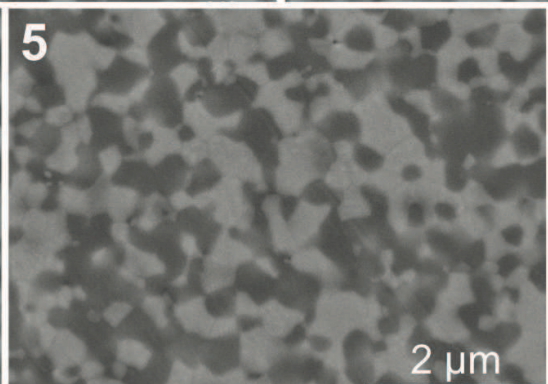


$341 \pm 7 \text{ nm}$



jace\_16335\_f4.eps

5



$321 \pm 10 \text{ nm}$

Author Manuscript

